

On the role of inertia and temperature in continuum and atomistic models of brittle fracture

This article has been downloaded from IOPscience. Please scroll down to see the full text article.

1998 J. Phys.: Condens. Matter 10 10529

(<http://iopscience.iop.org/0953-8984/10/47/004>)

View [the table of contents for this issue](#), or go to the [journal homepage](#) for more

Download details:

IP Address: 171.66.16.210

The article was downloaded on 14/05/2010 at 17:55

Please note that [terms and conditions apply](#).

On the role of inertia and temperature in continuum and atomistic models of brittle fracture

B N J Persson

IFF, FZ Jülich, D-52425 Jülich, Germany

Received 17 February 1998, in final form 7 August 1998

Abstract. Theoretical studies of crack motion in brittle materials often use continuum models where the relation between the crack velocity v and the driving force F is found to be continuous. However, for atomistic models the relation $v = v(F)$ is discontinuous and exhibits hysteresis. The difference is attributed to inertia, which is more important in atomistic models than in continuum models. I study the role of temperature in fracture dynamics and present a simple model study of the brittle-to-ductile transition.

There are several fundamental issues unsolved in the modern theory of fracture dynamics [1, 2]. The traditional approach to brittle fracture is to study continuum models. However, in continuum models the stress at the crack tip in an ideally brittle material (no plasticity) is singular (the stress varies as $\sim r^{-1/2}$ with the distance r from the crack tip). Since breaking individual bonds at the crack tip is the fundamental crack-growth mechanism in brittle fracture, it is not clear how accurate a continuum description of brittle fracture is. Another important difference between continuum and atomistic models is the role of inertia, which is more important in the atomistic models.

In this paper I study a very simple one-dimensional (1D) atomistic model of brittle fracture. Marder and co-workers [3] have studied the same model and solved it exactly for $T = 0$ using the Wiener–Hopf method. The results presented below extend their result to finite temperature. Furthermore, for $T = 0$ we present a comparison between the exact result and the result obtained using the continuum approximation, and emphasize the importance of inertia in the atomistic model. We also present a simple model study of the brittle-to-ductile transition.

We find that the transition from a stationary to a moving crack, as a function of the applied driving force, occurs continuously in the continuum model. In the atomistic model (at low temperatures) the transition is discontinuous and exhibits hysteresis as a function of the driving force. This difference is attributed to the absence of important inertia effects in the continuum model, and should also hold for more realistic 3D models [4, 3]. Thus, a crack is either pinned or it propagates with high speed (of the order of the sound velocity).

We consider the 1D model illustrated in figure 1. A string of atoms are connected by harmonic springs (spring constant k_1) to the upper surface of the ‘solid’ and to the lower part with springs (spring constant k_2) which, however, break when the vertical displacement of an atom exceeds some (atomic) length u_* . In addition, the string of atoms are connected to each other by springs with the bending force constant k_0 . We assume that $k_0 = k_2 \gg k_1$. The k_1 -springs represent (schematically) the long-range ‘elasticity’ of the upper part of the

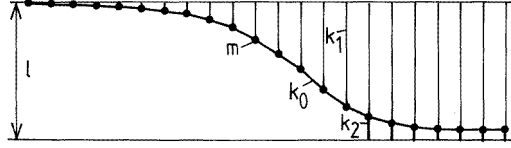


Figure 1. The one-dimensional model of a crack. The thin and thick vertical lines denote weak (spring constant k_1) and stiff (k_2) harmonic springs. The particles (black dots) of mass m are connected by stiff springs with the bending force constant k_0 .

‘solid’, i.e., $k_1 \sim E/W$ (where E is the elastic modulus and W the vertical width of the solid in figure 1).

The equation of motion for atom i is

$$m\ddot{u}_i + m\eta\dot{u}_i = k_0(u_{i+1} + u_{i-1} - 2u_i) + k_1(l - u_i) + g_i + f_i \quad (1)$$

where the force g_i is given by

$$g_i = -k_2u_i \quad \text{if } u_i < u_* \\ g_i = 0 \quad \text{if } u_i > u_*$$

and where f_i is a fluctuating force associated with the thermal motion of the atoms, which satisfies

$$\langle f_i(t)f_j(0) \rangle = 2m\eta k_B T \delta(t)\delta_{ij}. \quad (2)$$

The friction η is introduced in order to damp out the elastic waves emitted from the moving crack tip; in the calculations presented below we have chosen η very small. Let us introduce dimensionless variables. We measure length in units of u_* , time in units of $(m/k_0)^{1/2}$, energy in units of $E_0 = k_0u_*^2$ ($E_0/2$ is the bond energy) and the spring constant k_1 in units of k_0 . This gives

$$\ddot{u}_i + \eta\dot{u}_i = u_{i+1} + u_{i-1} - 2u_i + k_1(l - u_i) + g_i + f_i \quad (3)$$

where $g_i = -u_i$ if $u_i < 1$ and zero otherwise, and where

$$\langle f_i(t)f_j(0) \rangle = 2T\eta\delta(t)\delta_{ij}. \quad (4)$$

We have solved equations (3) and (4) by numerical integration, with the stochastically fluctuating force f_i obtained by adding many random numbers which are equally distributed in the interval between $-1/2$ and $1/2$. As an example, figure 2 shows the dependence on time of the position, $n(t)$, of the crack tip, for a 1000-atom chain. The initial crack extends from atom 1 to atom 400 and in the calculation we have used $k_1 = 0.01$ and $\eta = 0.03$. The external force acting on the crack is increased slowly by increasing l linearly with time from 8 at $t = 0$ to 15.5 at $t = 250$ (the vertical dotted line in figure 2), while l is kept constant at 15.5 for $t > 250$. Note the regular nature of the crack propagation; we have not observed any (oscillatory) instability in crack propagation for any driving force. This is consistent with the study of Langer [5], where the continuum version of model (1) was shown to have only stable steady-state propagating cracks.

In the continuum limit and for zero temperature, equation (3) takes the form

$$\ddot{u} + \eta\dot{u} = u'' + k_1(l - u) + g(u) \quad (5)$$

where $u' = \partial u(x, t)/\partial x$ and $\dot{u} = \partial u(x, t)/\partial t$. The model (5) differs from the model studied by Langer in that we use a different form for $g(u)$. Equation (5) has a solution corresponding

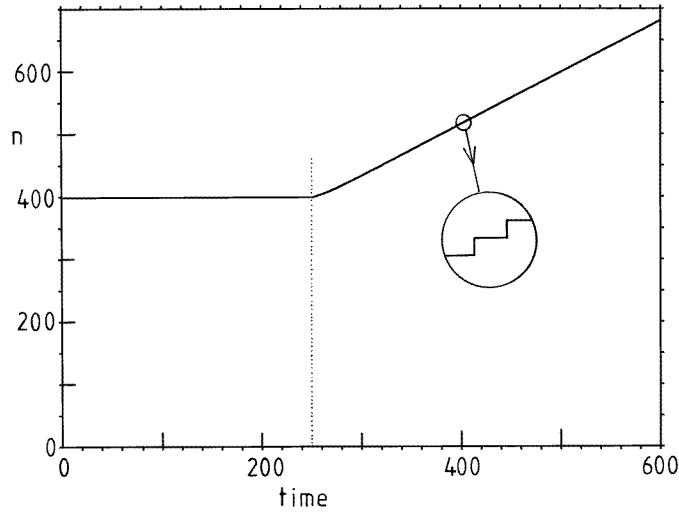


Figure 2. The position n of the crack tip as a function of time at zero temperature. The initial crack extends from atom 1 to atom 400. The applied stress is slowly increased by displacing the upper ‘surface’ in figure 1 from $l = 8$ at time $t = 0$ to 15.5 at $t = 250$ (the dotted vertical line). For $t > 250$, l is kept constant at 15.5. In the calculation we have used $\eta = 0.03$ and $k_1 = 0.01$. The inset shows the discontinuous changes in n associated with breaking the individual bonds.

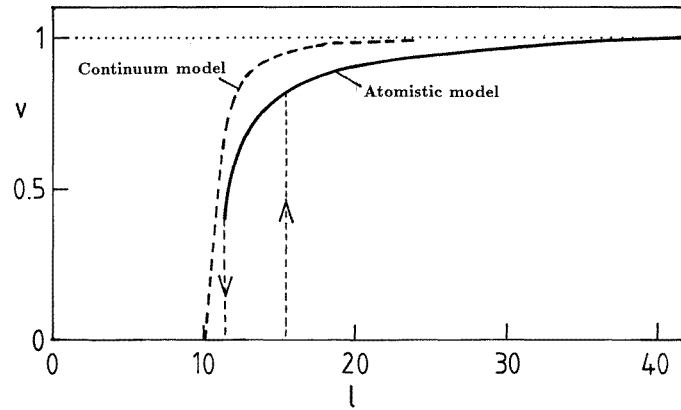


Figure 3. The relation between the crack velocity v and the displacement l for the continuum model (dashed line) and the atomistic model (solid line). The calculation is for $T = 0$ K with $\eta = 0.03$ and $k_1 = 0.01$.

to a crack which moves with the constant velocity v . Substituting $u(x, t) = u(x - vt)$ in (5) gives

$$(1 - v^2)u'' + \eta v u' + k_1(l - u) + g(u) = 0. \tag{6}$$

For $x > vt$ this equation reduces to

$$(1 - v^2)u'' + \eta v u' + k_1(l - u) - u = 0$$

with the general solution

$$u = Ae^{-\lambda(x-vt)} + \frac{k_1 l}{k_1 l + 1} \quad (7)$$

where

$$\lambda = \frac{\eta v}{2(1-v^2)} + \left[\left(\frac{\eta v}{2(1-v^2)} \right)^2 + \frac{k_1 + 1}{1-v^2} \right]^{1/2}. \quad (8)$$

For $x < vt$, equation (6) reduces to

$$(1-v^2)u'' + \eta v u' + k_1(l-u) = 0$$

with the solution

$$u = Be^{\mu(x-vt)} + l \quad (9)$$

where

$$\mu = -\frac{\eta v}{2(1-v^2)} + \left[\left(\frac{\eta v}{2(1-v^2)} \right)^2 + \frac{k_1}{1-v^2} \right]^{1/2}. \quad (10)$$

At the crack tip ($x = vt$), $u = 1$ which gives

$$A + k_1 l / (k_1 l + 1) = 1 \quad B + l = 1. \quad (11)$$

From the equation of motion (6) it follows that u' is continuous at $x = vt$ which gives

$$-\lambda A = \mu B. \quad (12)$$

Using (8), (10)–(12) gives

$$\left(\left[1 + \frac{4(1-v^2)(1+k_1)}{\eta^2 v^2} \right]^{1/2} + 1 \right) / \left(\left[1 + \frac{4(1-v^2)k_1}{\eta^2 v^2} \right]^{1/2} - 1 \right) = (l-1)(1+lk_1). \quad (13)$$

This relation between the crack velocity v and the displacement l , which is proportional to the driving force, is shown in figure 3. Note that $v = 0$ for $l < l_c$ (where $l_c \approx 10$), and that the transition from a stationary to a moving crack, as a function of the applied driving force (which is proportional to l), is *continuous*. On the other hand, for the atomistic model the transition is *discontinuous* and *exhibits hysteresis* as a function of the driving force (see figure 3). In particular, no steady crack motion is possible for velocity $v < v_c$, where $v_c \approx 0.4$. This gap of forbidden crack velocities is due to inertia, as can be understood as follows.

When the external driving force has increased to the point that the first atom–substrate bond breaks at the crack tip, the broken-off atom will initially accelerate upwards and, because of the finite atomic mass, *overshoot* the equilibrium position associated with a stationary crack. This implies that the force on the new crack-tip atom, for some short time interval, will be larger than for the stationary crack. Thus during crack propagation the effective driving force acting at the crack tip will be larger than the external driving force, resulting in a ‘high’ (steady-state) crack velocity v . Thus the transition from a stationary to a moving crack is discontinuous and will exhibit hysteresis as a function of the driving force.

In the continuum model, an infinitesimal strip of the elastic string will initially break off from the ‘substrate’. Since this segment of the string has a negligible mass, a negligible inertia force will be exerted on the part of the string which is bound to the substrate. Thus

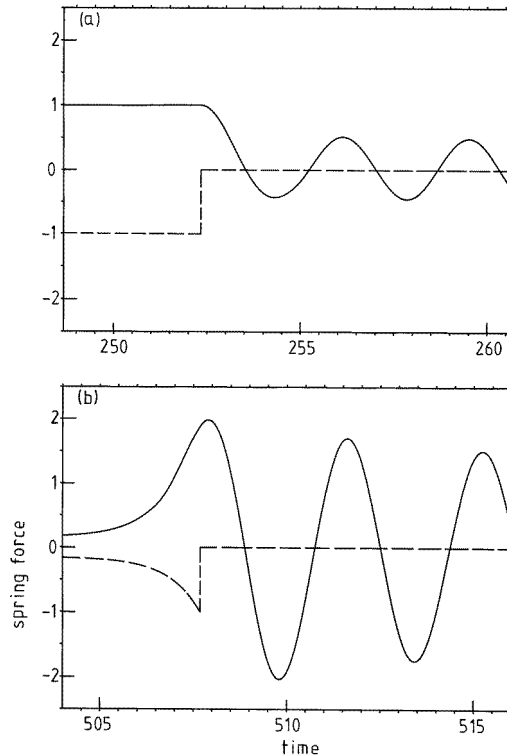


Figure 4. The time variation of the force acting on an atom from spring k_2 (dashed lines) and from springs k_0 and k_1 (solid lines). (a) For the atom at the initial crack-tip position ($n = 400$). (b) During steady-state crack motion ($n = 608$). The results refers to the calculation reported on in figure 2.

the crack tip will experience the same driving force as at the start of the crack motion, and the crack will propagate very slowly.

Let us study the effects of inertia in more detail. Figure 4 shows the time dependence of the upward (solid line) and downward (dashed line) spring forces acting on (a) atom $n = 400$ and (b) atom $n = 608$ in the simulation reported on in figure 2, as the crack tip passes the atoms. The former force is derived from the springs k_0 and k_1 , while the latter force is derived from the spring k_2 . In the calculation it is assumed that the driving force is just large enough to start crack motion ($l = 15.5$; see figure 3). Figure 4(a) shows the forces on the crack-tip atom at the initiation of crack motion. Before the crack starts to move, the upwards and downwards spring forces increase slowly and nearly balance each other, as they must when inertia effects are negligible (note: the external force is increased very slowly to its final value, corresponding to the displacement $l = 15.5$). When the force in the k_2 -spring reaches unity, this spring breaks, and the atom accelerates upwards. From here on, inertia effects are very important. After a short time interval, during which the crack tip accelerates, a steady state is reached where the crack propagates with a constant velocity. Figure 4(b) shows the time variation of the spring forces acting on an atom as the crack tip passes it during steady crack motion. In this case, owing to inertia, when the force in the k_2 -spring equals unity, the upward spring force is roughly twice as large as the force in the spring k_2 . That is, the effective driving force is much larger than the external

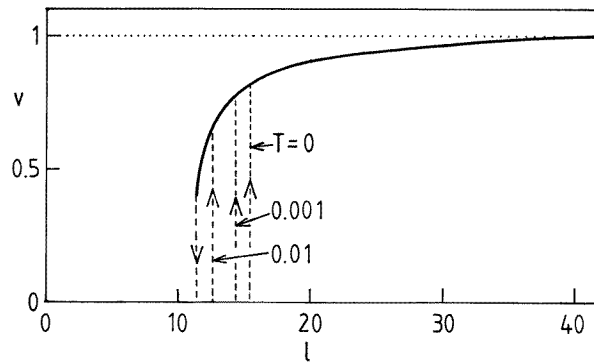


Figure 5. The temperature dependence of the relation between the crack velocity v and the displacement l for the atomistic model. For $\eta = 0.03$ and $k_1 = 0.01$.

driving force, and as a result the crack tip moves 'fast'.

Let us now discuss the influence of temperature on the hysteresis cycle in figure 3. Figure 5 shows the relation between the crack velocity v and the displacement l for the temperatures $T = 0, 0.001$ and 0.01 . Note that the onset of crack propagation decreases when the temperature increases. The physical origin of this effect is clear: even if the external force is below the value necessary to break the bond, for $T > 0$ a thermal fluctuation can break the (stretched) bond at the crack tip. When the bond is broken, inertia effects will increase the effective force acting on the crack tip which may induce the next bond to break. This 'chain reaction' will accelerate the crack until it finally reaches a steady state. Thus the higher the temperature, the smaller the hysteresis cycle. In addition, the longer the crack is exposed to external forces, the larger the chance will be that a large enough thermal fluctuation will occur, which will start crack motion (in the simulations in figure 5 the crack was studied for 600 time units). Thus the size of the hysteresis cycle (for $T > 0$ K) depends on the loading rate. When the temperature T is high 'enough' the relation between v and the driving force is continuous and exhibits no hysteresis. This is illustrated in figure 6 (thick dashed line) which shows v as a function of l when $T = 0.1$. In figure 7 we show the position $n(t)$ of the crack tip for $l = 10.5$ and 12 with $T = 0.1$. Note

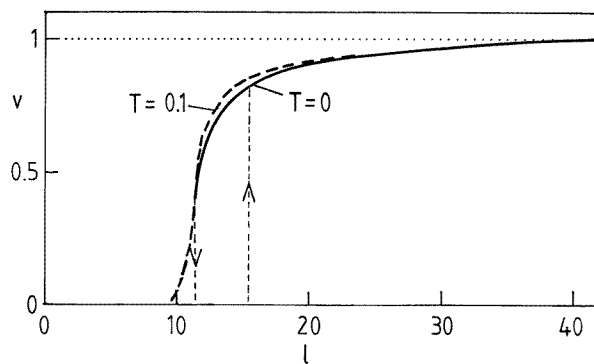


Figure 6. The dependence of the crack velocity on l for $T = 0$ (solid line) and for $T = 0.1$ (thick dashed line). For $\eta = 0.03$ and $k_1 = 0.01$.

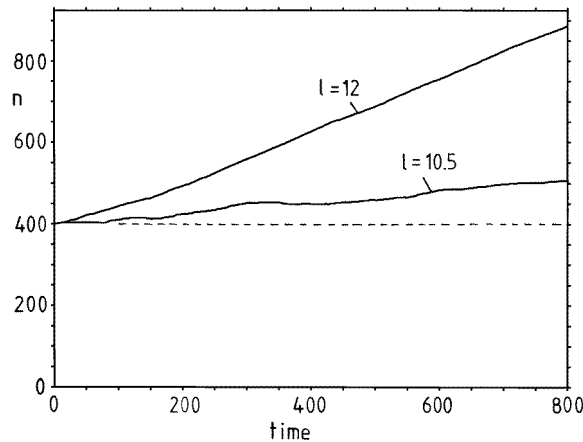


Figure 7. The position n of the crack tip as a function of time at $T = 0.1$ and for $l = 10.5$ and 12. The initial crack extends from atom 1 to atom 400. For $\eta = 0.03$ and $k_1 = 0.01$.

that for a ‘large’ driving force ($l = 12$) the fluctuations in n , which are due to the finite temperature, are very small. On the other hand, for $l = 10.5$ the fluctuations in $n(t)$ are relatively large, and for some short time intervals, $n(t)$ even decreases. At lower applied force this effect becomes even larger: the crack tip will perform a Brownian motion with only a slight drift in the direction of increasing crack length. We note, however, that in real systems the ‘backward’ jumps (which result in a decrease in the length of the crack) may not occur since the ‘fresh’ crack areas may immediately reconstruct, or the surface dangling bonds may rapidly react with foreign atoms, e.g., from the atmosphere. Finally, note that for real solids plastic deformations are usually important at high temperatures, but such effects are not included in the model studied above.

In the 3D case the crack tip is a line rather than a point. Due to the inhomogeneities which occur in most real materials, the crack tip will exhibit pinning forces which vary along the crack line. If the crack grows by a segment of the crack front jumping forward only to be stopped by a tougher region, then a point on the crack front a distance r away will initially ‘feel’ no change in stress. However, after a time period corresponding to the time $\sim r/c$ that it takes for the sound (Rayleigh) waves to propagate between the two points, the stress will temporarily increase at the second point on the crack line. Such *stress overshoot* can cause segments of the crack front to make a jump forwards that would not have been triggered by the static-stress changes. As with the atomic inertia effect discussed above, one can argue that this leads to an effective increase in the driving force and to a discontinuous onset of crack propagation and to hysteresis [6]. This effect should prevail in both continuum and atomistic models of brittle fracture.

The results above indicate that in ‘simple’ brittle solids at zero temperature, and in the absence of reactive foreign atoms and molecules, a crack is either pinned or moves rapidly with a speed of the order of the sound velocity. This result is inconsistent with the (often-made) assumption of a critical region where $v \sim (F - F_c)^\beta$ when the driving force F is above but close to the onset F_c force for crack propagation. However, slow crack motion can occur under three different conditions. Firstly, at sufficiently high temperature, the crack motion may be continuous (see figure 3). Secondly, stress corrosion may occur where the bonds at the crack tip are (irreversibly) broken by reaction with foreign atoms or molecules, e.g., from the surrounding atmosphere. This may lead to a slow ‘creep’ motion even if the

driving force is below F_c . Thirdly, in materials where the fracture energy is much larger than the surface energy of the surfaces created, large plastic or viscoelastic deformations occur in the vicinity of the crack tip, which may allow slow motion of the crack tip. This follows from the fact that large local energy dissipation at the crack tip reduces the importance of inertia effects (the motion may become ‘overdamped’) which makes slow crack motion possible. Thus, slow crack motion has been observed in model studies of the brittle fracture of polymers, where pulling out of the polymer chains leads to large energy dissipation [7]. Similar effects may occur in metals where large plastic deformations usually occur in the vicinity of the crack tip. These processes probably give rise to the slowly moving cracks that have been observed in many experiments, e.g., in polymers [8] and in soda-lime silica glasses and metallic alloys [9] (in the experiments in [9] the velocities were in the range $v = 10^{-9}$ – 10^{-7} m s $^{-1}$ and thermal activation must have played an important role). We also note that in many cases the surfaces of fractured materials exhibit a self-affine structure [9, 10], which can be naturally explained if the crack tip is assumed to obey an *overdamped* equation of motion (i.e., inertia is assumed negligible), with a random pinning potential arising from inhomogeneities in the solid [6, 11, 12].

Finally, let us briefly comment on the ductile-to-brittle transition. In simple atomistic solids, the local stress at a crack tip at the onset of brittle fracture is of order the bulk elastic modulus E . For most metals this is ~ 100 times larger than the stress necessary for plastic deformations. Thus one may think that large plastic deformations and ductile fracture rather than brittle fracture always occur for metals. However, this is not necessarily the case for the following reason. Plastic deformation in crystalline materials is due to the motion of pre-existing dislocations and the generation of new dislocations. Because of the finite concentration of dislocations and dislocation sources, it is very unlikely that a dislocation (or dislocation source) will occur right at an atomically sharp crack tip. Thus, if d is the average distance between two nearby dislocations, then one expects the distance between a crack tip and a nearby dislocation to be $\sim d$. Thus if the stress at the crack tip is $\sim E$, then the stress at the dislocation will be $\sim (a/d)^{1/2} E$ (where a is an atomic dimension), and if this is below the macroscopic yield stress $\sigma_c \sim E/100$, negligible plastic deformation is expected and brittle fracture will occur. However, time-dependent plastic flow (creep) can also occur as a result of thermal excitation even if the external stress is below that necessary for plastic deformation at zero temperature. Thus, a material which is brittle at ‘low’ temperatures may be ductile at ‘high’ temperatures. Similarly, since creep requires ‘long’ times to give rise to ‘large’ plastic flow, if a material is exposed to external forces which vary rapidly over time it may undergo brittle fracture, while ductile fracture may occur if the external forces change slowly with time.

Since dislocations usually have a large spatial extent, first-principles computer simulations of the brittle–ductile transition are essentially impossible with present-day computers [13]. However, one may use simple models to capture the essentials of the nature of this transition. We will illustrate this with the 1D model studied above. When local plastic flow occurs in the vicinity of the crack tip in a real material, it usually reduces the stress at the crack tip, and the externally applied stress must be increased to an even higher value before the local stress at the crack tip is high enough to break the local bonds. We can model this approximately by, instead of reducing the stress at the crack tip, strengthening the bond at the crack tip. Thus we allow the spring constant at the crack tip to vary with time: $k_2 \rightarrow h(t)k_2$ where $h(t)$ is determined as follows. The probability rate for plastic deformation is taken to be $w = \nu \exp(-\Delta E/k_B T)$ where the activation energy $\Delta E = \Delta E_0 - Au_i$ where ΔE_0 and A are constants. The probability P that plastic deformation will occur in a short time interval τ (taken to be the discretizing time period used in the integration of the equations

of motion (3)) is assumed to be $P = w\tau$. To take into account the stochastic nature of the thermal excitation over the barrier (leading to local plastic flow), we use random numbers to determine when the plastic deformation occurs. Thus, if r is a random number between zero and one, if $P > r$ plastic deformation is assumed to have occurred in the time interval τ , and $h(t)$ is increased by Δh . In the simulation presented below we have used $\Delta h = 0.1$, and (in the dimensionless units introduced earlier) $\nu = 100$ and $\Delta E = 0.6 - 0.5u_i$. Note that in this case no plastic flow can occur at zero temperature since $\Delta E > 0$ for $u_i = 1$.

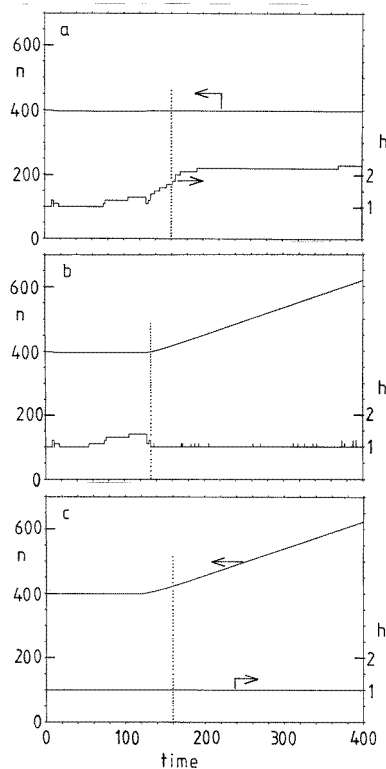


Figure 8. The position n of the crack tip and the strength h of the bond at the crack tip as functions of time. (a) For $T = 0.025$. The displacement l is increased linearly with time from $l = 8$ at $t = 0$ to $l = 16$ at $t = 160$ (the dotted vertical line) after which l is kept constant at $l = 16$. (b) As (a), but for a more rapid increase in l (from $l = 8$ to 16 when t increases from 0 to 133.33). (c) As (a), but with $T = 0.01$.

Figure 8 shows the results of three simulations when ‘plasticity’ is included according to the prescription outlined above. The position n of the crack tip and the strength h of the bond at the crack tip are shown as functions of time. In (a) the temperature $T = 0.025$. The displacement l is increased linearly with time from 8 at $t = 0$ to 16 at $t = 160$ (the dotted vertical line) after which l is kept constant at $l = 16$. In this case strong plastic deformation occurs and the crack tip is pinned. In (b) the external force is applied more rapidly than in (a) (l increases from 8 to 16 when t increases from 0 to 133.33) resulting in brittle fracture. Similarly, if the temperature is lowered below some critical temperature, brittle crack motion occurs. This is illustrated in (c) for $T = 0.01$ but with all of the other parameters the same as in (a).

References

- [1] Freund L B 1990 *Dynamic Fracture Mechanics* (New York: Cambridge University Press)
- [2] Fineberg J, Gross S P, Marder M and Swinney H L 1991 *Phys. Rev. Lett.* **67** 457
Sharon E, Gross S P and Fineberg J 1995 *Phys. Rev. Lett.* **74** 5096
- [3] Marder M and Liu X 1993 *Phys. Rev. Lett.* **71** 2417
Marder M and Gross S 1995 *J. Mech. Solids* **43** 1
- [4] Abraham F F, Brodbeck D, Rafey R A and Rudge W E 1994 *Phys. Rev. Lett.* **73** 272
- [5] Langer J S 1992 *Phys. Rev. A* **46** 3123
Ching E S C, Langer J S and Nakanishi H 1995 *Phys. Rev. E* **52** 4414
- [6] Fisher D S, Dahmen K, Ramanathan S and Ben-Zion Y 1997 *Phys. Rev. Lett.* **78** 4885
- [7] Persson B N J 1998 *Phys. Rev. Lett.* **81** 3439
- [8] Huntley J M 1990 *Proc. R. Soc. A* **430** 525
- [9] Daguir P, Nghiem B, Bouchaud E and Creuzet F 1997 *Phys. Rev. Lett.* **78** 1062
- [10] Bouchaud E 1997 *J. Phys. C: Solid State Phys.* **9** 4319
- [11] Nattermann T, Stepanow S, Tang L-H and Leschhorn H 1992 *J. Physique II* **2** 1483
- [12] Ertas D and Kardar M 1992 *Phys. Rev. Lett.* **69** 929
- [13] Carlsson A E 1997 *Solid State Physics* vol 51 (New York: Academic) p 233